**Applied Science, Computing and energy, 2025, 3(2):274-285**

# First-Principles $G_0W_0$+BSE Calculations: Electronic and Optical Properties of Zns Monolayer

**Ibrahim Bashir Usman, Auwalu Musa*, Abdullahi Lawal, Aliyu Muhammad**
**Received: 02 July 2025/Accepted: 27 August 2025/Published online: 05 September 2025**

*Abstract: We investigated the electronic structure and optical properties of 2D graphene-like wurtzite ZnS using first-principles calculations and many-body perturbation theory (MBPT). The structural properties were determined through first-principles calculations based on density functional theory (DFT). Structural optimization yields lattice constants of 3.81 Å for bulk and 3.76 Å for the monolayer, with Zn–S bond lengths of 2.33 Å and 2.21 Å, respectively and these values are in good agreement with experimental results. The quasiparticle band structure, excitonic, and optical properties were computed using many-body perturbation theory (MBPT) within one-shot GW ($G_0W_0$) approximation and the Bethe-Salpeter equation (BSE) approach, specifically $G_0W_0$-BSE. The electronic properties results show that ZnS sheet exhibits a direct band gap at the Γ-point, which remains unchanged as a direct semiconductor when electron-electron interactions are considered. The $G_0W_0$ calculations verify that monolayer ZnS is a direct bandgap material with a bandgap value of 4.106 eV, which is consistent with experimental findings. The results of optical properties with inclusion of electron-hole interactions revealed that monolayer ZnS has exciton energy of 3.66 eV with binding energy of ~0.95 eV. The strong excitonic effects in the ZnS monolayer sheet make it promising for optoelectronic device* applications.

***Keywords:*** *ZnS, monolayer, DFT, $G_0W_0$, $G_0W_0$+BSE, Optoelectronic*

**Ibrahim Bashir Usman**
**Address:** Department of Physics, Bayero University, Kano, Kano State, Nigeria
**Ema**il:**ibrahimbashir26@yahoo.com**
**Orcid id: https://orcid.org/0009-0006-9681-1853**

**Auwalu Musa**
**Address:** Department of Physics, Bayero University, Kano, Kano State, Nigeria
**Email:amusa.phy@buk.edu.ng**

**Abdullahi Lawal**
Department of Physics, Ahmadu Bello University, Zaria, Kaduna State, Nigeria
**Email:abdullahikubau@yahoo.com**
**Orcid id: https://orcid.org/0000-0003-1294-3180**

**Aliyu Muhammad**
Department of Physics, Ahmadu Bello University, Zaria, Kaduna State, Nigeria
**Email: aliyumuhammad93@gmail.com**

## 1.0 Introduction

Research on semiconductor materials with different crystalline phases has been a key driver of the development of modern electronic and optoelectronic applications. Among these materials, zinc sulfide (ZnS) exhibits polymorphism, mainly existing in the cubic zinc blende (zb-ZnS) and hexagonal wurtzite (wz-ZnS) structures (Shahrokhi, 2016), each demonstrating distinctive structural and electronic properties. The wurtzite phase of ZnS, which is characterized by hexagonal lattice structure, presents a slight but critical difference in atomic coordination and lattice structure compared to its cubic counterpart, which has a major influence on the electronic and optical properties of the ZnS molecule. The most important application of ZnS is in light-

emitting diodes, lasers, flat-panel displays, and photocatalysts (Majidiyan Sarmazdeh et al., 2017). ZnS is a semiconductor with a direct bandgap (Eg = 3.72 eV in the cubic zinc blend phase and Eg = 3.77 eV in the hexagonal wurtzite phase) that promises a number of novel applications (Sharma et al., 2019). The choice of structure, size and dimension (bulk versus monolayer) has a significant influence on its properties. In recent years, the 2D monolayer form of ZnS has been attracting increasing interest because of its potential for novel electronic and optical applications. Although the monolayer of ZnS has not been synthesized yet, thin film ZnS with thickness of 11 Å in wurtzite phase have been synthesized (Majidiyan Sarmazdeh et al., 2017). The electronic transition between the valence band (VB) and conduction band (CB) produces optical properties, like photoluminescence (PL) emission and absorption. The reduced dimensionality of the material significantly impact on the electronic structure of these bands (Kumbhakar et al., 2021). Also, the interaction of materials with optical waves and photons is strongly dependent on the structure, which can then be used to control light field distribution and light propagation (Flory, 2011). Similarly, change in dimension show enhanced electronic and optoelectronic properties. Density Functional Theory (DFT) provides a computational approach to investigate these properties by allowing for the calculation of the structural, electronic properties as well as optical spectrum based on atomic structure. These theoretical insights provide the basis for interpreting experimental data and customizing the properties of materials for optoelectronic applications. within DFT, the Generalized Gradient Approximation (GGA), especially the Perdew–Burke–Ernzerhof (PBE) functional (John P. Perdew, Kieron Burke, 1966), provides a balance between computational efficiency and reasonable accuracy. However, a known limitation of GGA-based functionals is the systematic underestimation of semiconductor band gaps. This shortfall arises primarily from the self-interaction error and the insufficient treatment of exchange–correlation interactions (John P. Perdew, Kieron Burke, 1966), (Becke, 1993).

Sharma et al., (2019) analyzed wz-ZnS and zb-ZnS using GGA, The reported band gaps was 2.06eV and 2.01eV, for wz-ZnS and zb-ZnS respectively, indicating significant underestimation of around 45% comparing to the experimental values of 3.72 eV for zb and 3.77 eV for wz-ZnS (Ves et al., 1990; Karazhanov et al., 2006; Voigt et al., 2020) reported that the GGA-calculated band gap for bulk ZnS was 2.03eVand this value is smaller than the experimental value. Conversely, the application of GGA+U adjusted the band gap to 3.57eV, illustrating the impact of adding on-site Coulomb interaction corrections. Similarly, in monolayer forms of ZnS, GGA functionals often yield band gaps in the range of 2.27–2.65eV (Lashgari et al., 2016), (Shahrokhi, 2016). These values are improved by adopting functionals such as $G_0W_0$ approximations, which can correct the band gap to values more consistent with experimental data. These investigations highlight in general the shortcomings of standard DFT-GGA in accurately estimating the band gap of ZnS and the effectiveness of using corrections for achieving results more closely corresponding to experimental observations. Understanding and addressing these inconsistencies are critical for the design and application of ZnS-based materials in optoelectronic devices.

For decades, researchers have used standard density functional theory (DFT) and the GW approximation to study the optical properties of materials (Gilmore et al., 2015; Lawal et al., 2021). However, these methods have limitations, particularly in describing excitonic effects and electron-hole interactions, which are crucial for accurate optical spectra predictions. The mentioned approaches often

yield significant discrepancies with experimental results (Li et al., 2024; Yusuf et al., 2024). To overcome this, a two-particle approach by solving Bethe-Salpeter equation (BSE) based on GW corrections can be employ. This method provides a more accurate description of optical properties, capturing the influence of electron-hole interactions and yielding results in better agreement with experimental data.

This study presents calculations of the structural properties of ZnS in monolayer using various exchange-correlation potentials within the framework of density functional theory (DFT) as implemented in Quantum Espresso. Additionally, electronic and optical properties are investigated using many-body perturbation theory (MBPT) via one-shot $G_0W_0$ approach and the solution of the Bethe-Salpeter equation (BSE), as implemented in the YAMBO package (Marini et al., 2009). The understanding of the electronic and optical properties of ZnS monolayers using G0W0+BSE will provide crucial theoretical insights for designing next-generation optoelectronic devices and guide future experimental synthesis of 2D ZnS materials

## 2.0 Computational Methods

The calculations were performed using the first principle methods based on DFT with plane wave as the basis set as implemented in the Quantum ESPRESSO (Open Source package for research in electronic structure, simulation and optimization, QE) simulation package (Giannozzi et al., 2009) and Many Body Perturbation Theory within GW approximation as implemented in YAMBO code (Marini et al., 2009). In the DFT calculation, exchange-correlation functional was approximated by the Generalized Gradient Approximation of Perdew–Burke–Ernzerhof (GGA-PBE) (John P. Perdew, Kieron Burke, 1966), to treat electron-electron interaction. First, the initial structure of bulk wurzite-structured Zinc Sulfide (wz-ZnS) was obtained from materials project of (Jain et al., 2013) and optimized using variable-cell relaxation (vc-relax), using GGA-PBE method. Then, a 7×7×1 k-points for the integration of the first Brillouin zone was chosen, while denser values of 12×12×1 were used for the density of states using a technique known as Marzarri-Venderbilt smearing. Plane waves with kinetic energy cutoffs of 50Ry to expand the electronic wavefunctions and 320Ry for charge density was used. Five other exchange correlations functional (BP, WC, PZ, PBE-sol and revPBE) were used to calculate the band structure. A vacuum layer of 20 Å was used in perpendicular direction (c-axis) of ZnS monolayer along the z-direction to avoid inter layer interaction. However, to correct the electronic band structure obtained from standard DFT approach, we performed GW calculations within $G_0W_0$ approximation as implemented in YAMBO package (Marini et al., 2009) to obtain a real quasiparticle (QP) energies (Eq.1) correction to the Kohn-Sham (KS) eigenvalues $E_{nk}^{DFT}$ (Lucarini et al., 2005).

$$E_{nk}^{QP} = Z_{nk}\langle\varphi_{nk}^{DFT}|\Sigma_{GW}(E_{nk}^{DFT}) - V_{XC}|\varphi_{nk}^{DFT}\rangle + E_{nk}^{DFT} \quad (1)$$

where $V_{XC}$ is the DFT exchange-correlation potentials, $\Sigma_{GW}$ is the GW self-energy which is the product of one-particle Green's function, G and screened Coulomb potential, and $k$ and $n$ are the k-point and band indices respectively, $E_{nk}^{DFT}$ and $\varphi_{nk}^{DFT}$ are the KS eigenvalues and eigenfunctions respectively, and $Z_{nk}$ is the orbital renormalization factor.

For calculating excitonic and optical properties using YAMBO, the Kohn-Sham (KS) energies and wave-functions from DFT calculations serve as input for the Bethe-Salpeter equation (BSE) calculations. The BSE is then solved using the Tamm-Dancoff approximation and interaction kernel, which accounts for dynamic screening and electron-hole interactions. This yields electron-hole interaction and excitation energies. Finally, the optical absorption spectrum is calculated, including the effects of electron-hole interactions, providing a more

accurate representation of the material's optical properties. On the other hand, for optical properties calculations, the dielectric function, $\varepsilon(\omega) = \varepsilon_1(\omega) + i\varepsilon_2(\omega)$, is investigated in terms of incident photon energy using random phase approximation (RPA). The real and imaginary parts of the dielectric function are denoted by $\varepsilon_1(\omega)$ and $\varepsilon_2(\omega)$, respectively (Lawal et al., 2017a), (Arbi et al., 2012).

$$\varepsilon_1(\omega) = 1 + \frac{2P}{\pi}\int_0^{\infty}\frac{\omega'\varepsilon_2(\omega')}{\omega'^2-\omega^2}d\omega' \qquad (2)$$

$$\varepsilon_2(\omega) = \frac{16\pi e^2}{\omega^2}\sum_s |\vec{\lambda}\langle O|\vec{v}|S\rangle|^2\delta(\omega-\Omega^s) \qquad (3)$$

where $\vec{\lambda}$ is the polarization vector of light $\langle O|\vec{v}|S\rangle$ is the optical transition matrix from valence to conduction states and is the principal value of the integral and the integral is over irreducible Brillouin zone. Understanding both the real and imaginary components of the dielectric function enables the calculation of optical properties. We calculated the refractive index $n(\omega)$, the extinction coefficient $k(\omega)$, the absorption coefficient $\alpha(\omega)$, the reflectivity $R(\omega)$, loss function $L(\omega)$, and the conductivity $\sigma(\omega)$ using the following equations (Arbi et al., 2012):

$$n(\omega) = \sqrt{\left(\frac{\sqrt{\varepsilon_1^2(\omega)+\varepsilon_2^2(\omega)}+\varepsilon_1(\omega)}{2}\right)} \qquad (4)$$

$$k(\omega) = \sqrt{\left(\frac{\sqrt{\varepsilon_1^2(\omega)+\varepsilon_2^2(\omega)}-\varepsilon_1(\omega)}{2}\right)} \qquad (5)$$

$$\alpha(\omega) = \frac{\omega}{c}\sqrt{2\left(\sqrt{\varepsilon_1^2(\omega)+\varepsilon_2^2(\omega)}-\varepsilon_1(\omega)\right)} \qquad (6)$$

$$R(\omega) = \left|\frac{\sqrt{\varepsilon(\omega)}-1}{\sqrt{\varepsilon(\omega)}+1}\right|^2 \qquad (7)$$

$$L(\omega) = \frac{\varepsilon_2(\omega)}{\varepsilon_1^2(\omega)+\varepsilon_2^2(\omega)} \qquad (8)$$

$$\sigma(\omega) = \frac{\omega\varepsilon_2(\omega)}{4\pi} \qquad (9)$$

## 3.0 Result and discussions

### *3.1 Structural properties*

The crystal structures of bulk and monolayer ZnS were optimized using density functional theory as implemented in Quantum ESPRESSO. Geometry relaxation was performed until the atomic forces were reduced below $1\times10^{-3}$ Ry/Bohr, and the total energy difference between iterations was less than $1\times10^{-6}$ Ry. For the bulk zinc wurtzite ZnS, the calculated equilibrium lattice constant was 3.81 Å, which compares well with the reported experimental value of about 3.82 Å (Kushwah et al., 2020) and theoretical work (Lashgari et al., 2016). The corresponding Zn–S bond length was obtained as 2.33 Å. In the case of the ZnS monolayer, a vacuum gap of about 20 Å was added along the out-of-plane direction to prevent spurious interactions between periodic images. After structural relaxation, the in-plane lattice constant was optimized to 3.76Å, with a Zn–S bond length of 2.21 Å. Compared with the bulk phase, the monolayer shows slightly shorter bond lengths, which can be attributed to reduced atomic coordination and stronger in-plane bonding. These findings are consistent with earlier theoretical reports (Behera & Mukhopadhyay, 2014), (Majidiyan Sarmazdeh et al., 2017). Fig. 1 shows the structures of bulk and monolayer ZnS, the comparison between bulk and monolayer ZnS reveals that reducing the dimensionality results in a modest contraction of both the lattice constant and Zn–S bond length. These structural variations are expected to influence the electronic band gap and optical absorption edge, which will be analyzed in the subsequent sections.

### *3.2 Electronic properties*

To investigate electronic properties of *Wz*-ZnS, the band structure, total and partial density of states (DOS) are calculated. Fig. 3 illustrate the band structures along the high symmetry Γ-M-K-Γ directions using different exchange correlation functionals and $G_0W_0$ approaches,

the electronic band structures were computed within six different exchange correlation approximations based on DFT in the energy range of -5 to 6eV setting Fermi energy level scale at 0eV represented by a red dash.

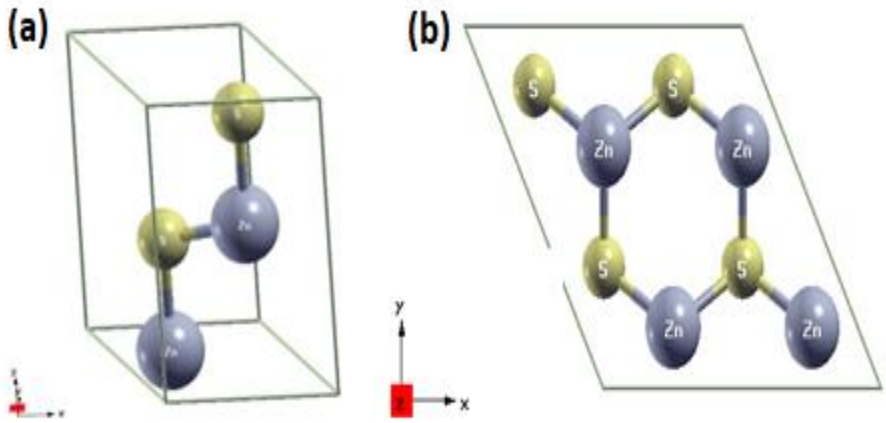


**Fig 1 Structure of ZnS: (a) Bul (b) Monolayer**

The obtained results are compared in table 1. Both the valence band maximum (VBM) and the conduction band minimum (CBM) for all funtionals occur at the Γ-point, resulting in a direct band gap. All the band gaps values obtained with the six exchange correlations are significantly smaller than experimental value. This discrepancy arises from the limitations of the DFT approach due to the approximations used in describing exchange-correlation functional. The discrepancy between DFT-predicted band gaps and experimental values can be addressed by incorporating many-body perturbation theory (GW) into DFT calculations. This approach utilizes the Green's function to accurately capture the electronic density of the fully interacting system, leading to improved band gap predictions. To accurately predict quasiparticle energies and band gaps, we applied self-energy corrections using the one-shot $G_0W_0$ approximation within many-body perturbation theory (MBPT). The resulting $G_0W_0$ band structure is shown in Fig. 2(g), providing a more reliable result of the material's electronic properties. As shown in Fig. 2(b), incorporating self-energy corrections via MBPT leads to a moderate band gap increase, resulting in better agreement with experimental values. The calculated direct quasiparticle band gap of monolayer ZnS is 4.106 eV. Our calculations reveal that the $G_0W_0$ approximation on top of standard DFT, accurately predicts the magnitude of the monolayer ZnS band gap. A comparison of our results with previous works are presented in Table 2.

### *3.2.1 Density of states*

To clearly understand the nature of the bands in monolayer ZnS. The total (TDOS) and projected density of states (PDOS) were calculated. The TDOS and PDOS (for rev-PBE functional only) are presented in Figure 3 (a) and (b) respectively, along with the Fermi energy level scale at 0 eV shown in a red dash. The main contribution of lowest valence band (the energy range between -14 and -6eV) is related to the Zn–d orbital, the main contribution of states in the maximum occupied valence bands (the energy range between -7eV to Fermi level) is related to S atom p-orbital and contribution of states in the conduction region (above 1 eV) is related to Zn-s orbital. Thus, for monolayer ZnS, the S atom p-orbital has the highest contribution in valence bands, while Zn atom s-orbital has the highest contribution in conduction bands.

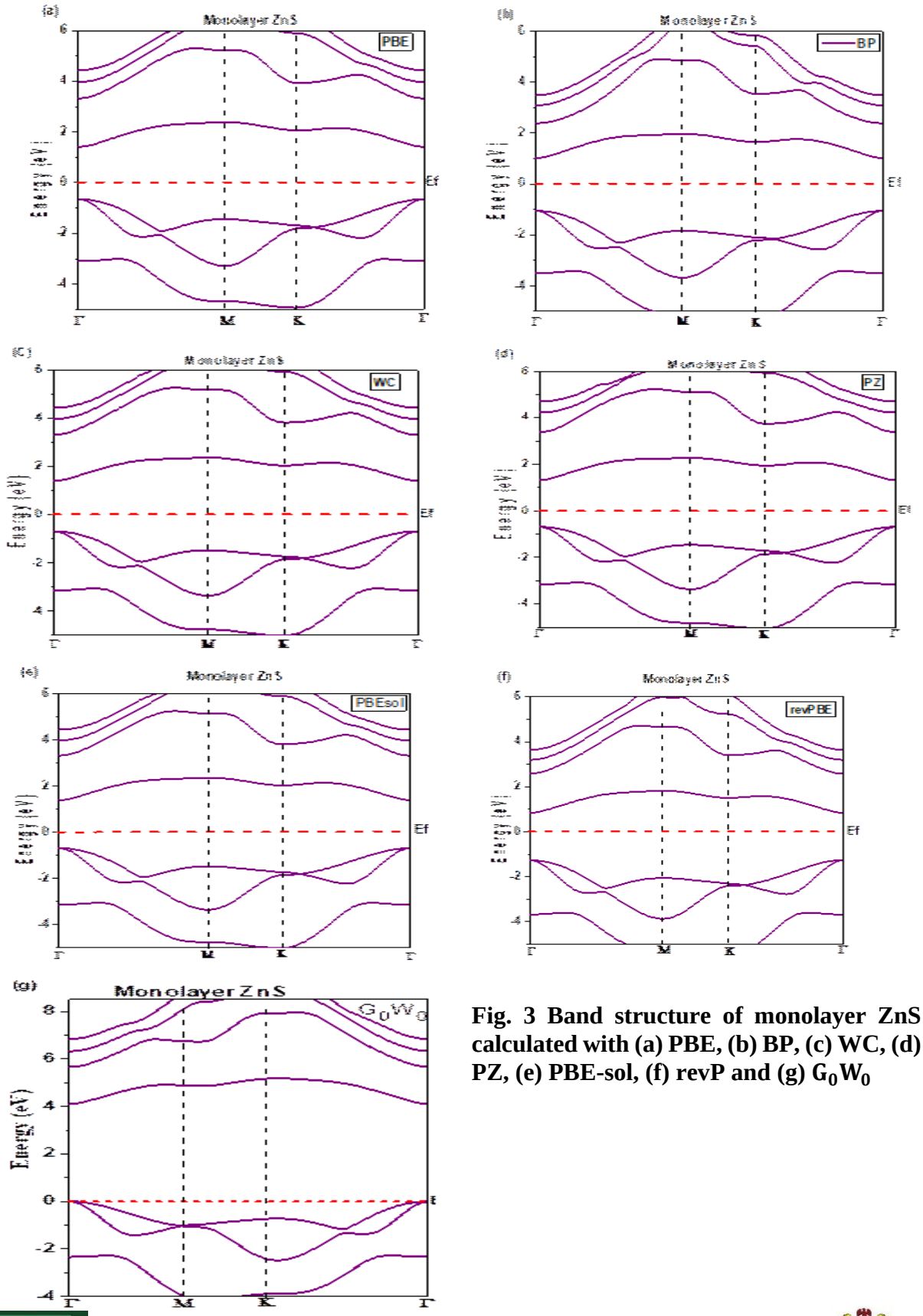


**Fig. 3 Band structure of monolayer ZnS calculated with (a) PBE, (b) BP, (c) WC, (d) PZ, (e) PBE-sol, (f) revP and (g) $G_0W_0$**

**Table 2: Comparison of energy band gap (eV) values calculated with local density approximation (LDA), generalized gradient approximation (GGA) and $G_0W_0$ results for monolayer ZnS**

| Methodology | Band Gap (eV) | Type of Gap |
|---|---|---|
| **PBE** | 2.070 | Direct |
| **BP** | 2.082 | Direct |
| **WC** | 2.104 | Direct |
| **PZ** | 2.014 | Direct |
| **PBEsol** | 2.086 | Direct |
| **revPBE** | 2.112 | Direct |
| **$G_0W_0$** | 4.106 | Direct |
| **Previous Theoretical Work** | | |
| **GGA (Shahrokhi, 2016)** | 2.650 | Direct |
| **GGA (Lashgari et al., 2016)** | 2.270 | Direct |
| **LDA (Behera & Mukhopadhyay, 2014)** | 2.622 | Direct |

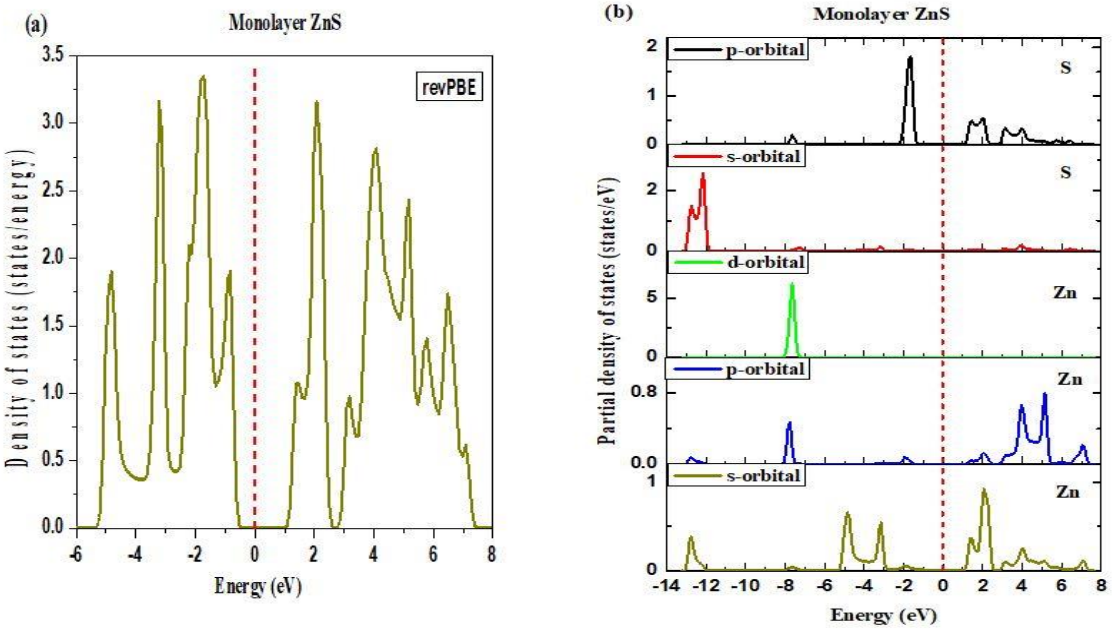


**Fig. 5 (a) Total density of state and (b) Partial density of states of Monolayer ZnS.**

### *3.3 Optical properties*

The optical properties of ZnS were studied using a combination of **Quantum ESPRESSO** and **YAMBO**. First, ground-state electronic structure calculations were performed using Quantum ESPRESSO within the generalized gradient approximation (GGA). The resulting Kohn-Sham wavefunctions were then used as input for optical property calculations in YAMBO. The optical response of the material was first analyzed by examining its dielectric function. Fig. 4(a) and (b) represent the real and imaginary part of dielectric function of monolayer ZnS for polarization along a parallel direction to the hexagonal axis. The imaginary part of the dielectric function, $\varepsilon_2(\omega)$, computed

by G₀W₀+RPA, reveals the absorption threshold around the quasiparticle gap, coupled with a broad feature signifying interband transitions. However, it does not account for the excitonic effects needed in two-dimensional materials. When excitonic effects are included by solving Bethe–Salpeter Equation (BSE) in addition to G₀W₀, the optical spectrum changes significantly. A strong peak of 3.66 eV appears below the quasiparticle band gap, which clearly indicates the presence of tightly bound excitons. The energy difference between this exciton peak and the band gap gives an estimated exciton binding energy of about 0.950 eV. The binding energy of the lowest energy exciton (EB) was computed by (Shahrokhi, 2016);

$$E_B = E_g - E_{ex} \quad (10)$$

where $E_g$ is the QP band gap and $E_{ex}$ is excitation energy. This result confirms that weak dielectric screening in 2D materials enhances excitonic interactions.

The real part of the dielectric function reflects how the material responds to an external electric field. Dielectric constant at higher frequency in the perpendicular direction $\varepsilon_\perp(\infty)$ for ($G_0W_0$ + BSE) is around 1.73; it reaches a peak at 4.14 eV near the absorption onset and decreases gradually at higher photon energies. For ($G_0W_0$+ RPA) approach, the dielectric constant start rising at 1.63. The static dielectric constant is found to be higher when excitonic effects are included, due to stronger polarization.

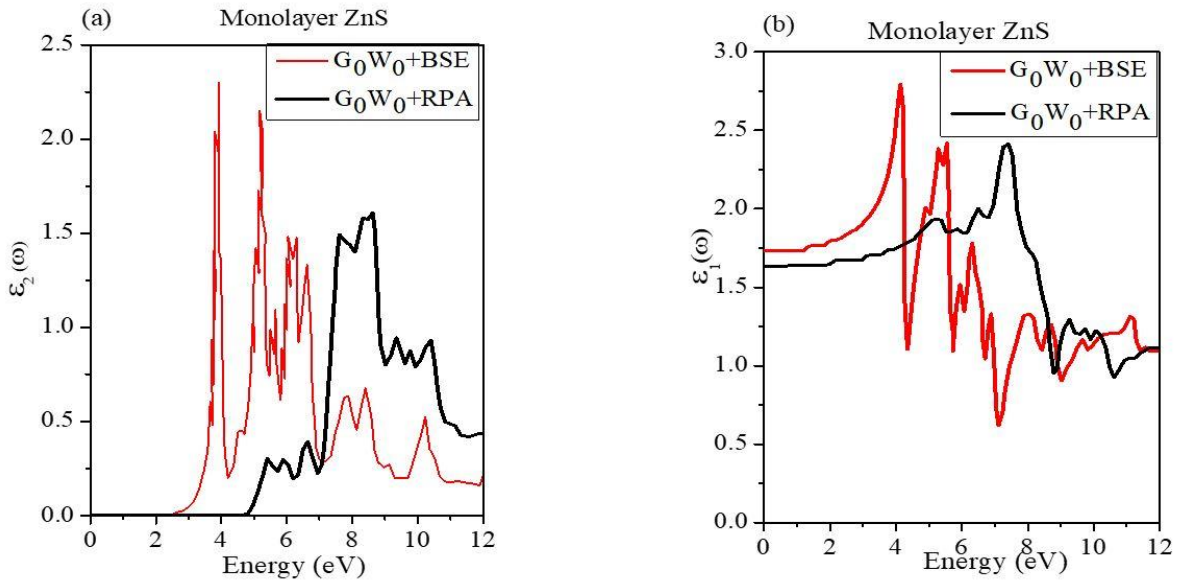


**Fig. 4 (a) Imaginary part of the dielectric function (b) Real part of the dielectric function of monolayer ZnS calculated using $G_0W_0$ + RPA and $G_0W_0$ + BSE**

The optical refractive index n(ω), derived from the dielectric function, help describe the material's interaction with light. Fig 5(a) and (b) shows the refractive index n(ω) and reflectivity R(ω) of monolayer ZnS as function of energy. The static refractive index is slightly higher in the $G_0W_0$+BSE case, reflecting an increased ability to slow down light. n(ω) rise steeply at lower photon energies, attains high refractive index of 1.59 within UV region and decline at higher energies, consistent with the observed absorption behavior. The reflectivity R(ω) spectrum reveals how much light is reflected at different photon energies. From Fig 4(b), the spectrum is relatively low in the visible and near-UV range, the first edge with $G_0W_0$+BSE was found to be 4.573%. The

reflectivity spectrum starts to increase from 4.573%, attaining maximum level of 30.859% corresponding to photon energy value 6.826 eV, suggesting the material is largely transparent at those energies. Also, the value reflectivity spectrum at zero energy using $G_0W_0$+RPA was 1.291%. The low reflectivity across the entire spectrum makes the material suitable for applications that require high transparency or minimal reflection.

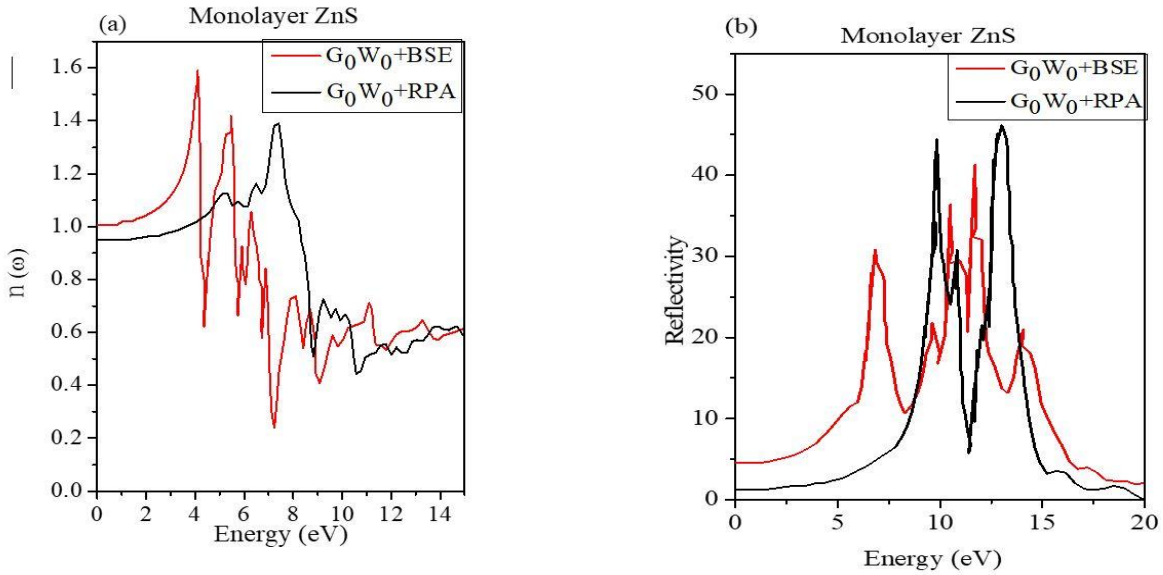


**Fig. 5 (a) Refractive index (b) Reflectivity of monolayer ZnS calculated using $G_0W_0$ + RPA and $G_0W_0$ + BSE.**

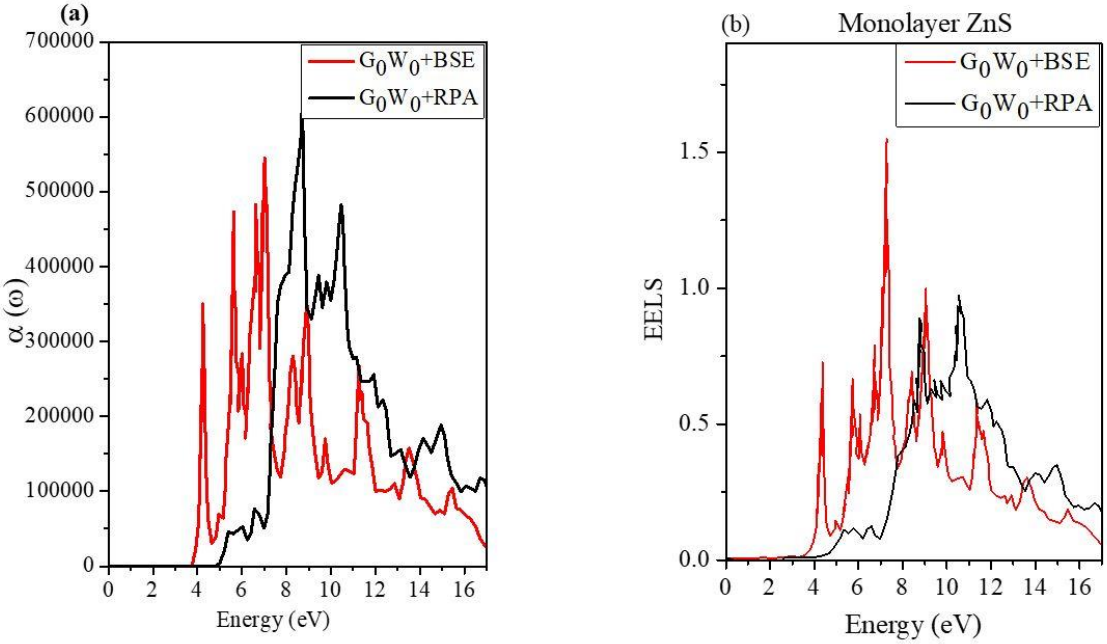


**Fig. 6 (a) Absorption coefficient (b) Electron Energy Loss Spectrum (EELS) of monolayer ZnS calculated using $G_0W_0$ + RPA and $G_0W_0$ + BSE.**

The absorption coefficient α(ω) provides insight into how effectively the material absorbs light across different energies. Fig 6(a) displays the absorption coefficient of monolayer ZnS in two approaches. In the $G_0W_0$+RPA spectrum, absorption starts around the corrected band gap and spans a broad range into the ultraviolet. After accounting for electron–hole interactions through the BSE, a pronounced peak appears just below the absorption edge at around 3.92 eV. The absorption edge is also slightly shifted to higher energy compared to previous DFT result. The electron energy loss function L(ω) reveals where collective excitations, or plasmons, occur. With the two approaches shown in Fig. 6, a clear peak for $G_0W_0$+BSE appears at the energy 7.27 eV, consistent with (Shahrokhi, 2016), signaling a plasmon resonance. This feature remains mostly unaffected by the inclusion of excitonic effects, as it arises from higher-energy collective motions rather than individual electron-hole transitions.

## 4.0 Conclusion

In conclusion, our comprehensive investigation of the electronic structure and optical properties of 2D graphene-like wurtzite ZnS using first-principles calculations and many-body perturbation theory (MBPT) has provided valuable insights into the material's potential applications. The calculated lattice constants and Zn–S bond lengths are in good agreement with experimental results, validating the accuracy of our DFT-based structural optimization. The quasiparticle band structure and excitonic properties computed using the G0W0-BSE approach reveal that monolayer ZnS is a direct bandgap material with a bandgap value of 4.106 eV, consistent with experimental findings. The strong excitonic effects, characterized by an exciton energy of 3.66 eV and a binding energy of ~0.95 eV, make monolayer ZnS a promising candidate for optoelectronic device applications. These results demonstrate the potential of 2D ZnS in advancing optoelectronic technologies and highlight the importance of considering many-body interactions in understanding the material's properties.

## 5.0 References

Arbi, M., Benramdane, N., Kebbab, Z., Miloua, R., Chiker, F., & Khenata, R. (2012). First principles calculations of structural, electronic and optical properties of zinc aluminum oxide. *Materials Science in Semiconductor Processing, 15, 3,* pp. 301–307. https://doi.org/10.1016/j.mssp.2012.03.010.

Becke, A. D. (1993). Density-functional thermochemistry. III. The role of exact exchange. *The Journal of Chemical Physics, 98, 7,* pp. 5648–5652. https://doi.org/10.1063/1.464913

Behera, H., & Mukhopadhyay, G. (2014). Tailoring the structural and electronic properties of a graphene-like ZnS monolayer using biaxial strain. *Journal of Physics D: Applied Physics, 47, 7,* 075302. https://doi.org/10.1088/0022-3727/47/7/075302

Flory, F. (2011). Optical properties of nanostructured materials: A review. *Journal of Nanophotonics, 5, 1,* 052502. https://doi.org/10.1117/1.3609266

Giannozzi, P., Baroni, S., Bonini, N., Calandra, M., Car, R., Cavazzoni, C., Ceresoli, D., Chiarotti, G. L., Cococcioni, M., Dabo, I., Dal Corso, A., De Gironcoli, S., Fabris, S., Fratesi, G., Gebauer, R., Gerstmann, U., Gougoussis, C., Kokalj, A., Lazzeri, M., … Wentzcovitch, R. M. (2009). QUANTUM ESPRESSO: A modular and open-source software project for quantum simulations of materials. *Journal of Physics: Condensed Matter, 21, 39,* 395502. https://doi.org/10.1088/0953-8984/21/39/395502

Gilmore, K., Vinson, J., Shirley, E. L., Prendergast, D., Pemmaraju, C. D., Kas, J.

J., … Rehr, J. J. (2015). Efficient implementation of core-excitation Bethe–Salpeter equation calculations. *Computer Physics Communications*, *197*, pp. 109–117. https://doi.org/10.1016/j.cpc.2015.08.018.

Jain, A., Ong, S. P., Hautier, G., Chen, W., Richards, W. D., Dacek, S., Cholia, S., Gunter, D., Skinner, D., Ceder, G., & Persson, K. A. (2013). Commentary: The Materials Project: A materials genome approach to accelerating materials innovation. *APL Materials*, *1*, *1*, 011002. https://doi.org/10.1063/1.4812323

Perdew, J. P., Burke, K., & Ernzerhof, M. (1996). Generalized gradient approximation made simple. *Physical Review Letters*, *77*, *18*, pp. 3865–3868. https://doi.org/10.1103/PhysRevLett.77.3865

Karazhanov, S. Z., Ravindran, P., Kjekshus, A., Fjellvåg, H., Grossner, U., & Svensson, B. G. (2006). Coulomb correlation effects in zinc monochalcogenides. *Journal of Applied Physics*, *100*, *4*, 043709. https://doi.org/10.1063/1.2227266

Kumbhakar, P., Chowde Gowda, C., & Tiwary, C. S. (2021). Advance optical properties and emerging applications of 2D materials. *Frontiers in Materials*, *8*, 721514. https://doi.org/10.3389/fmats.2021.721514

Kushwah, N., Wadawale, A., Kedarnath, G., Sudarsan, V., & Kadam, R. M. (2020). Low temperature synthesis of wurtzite form of ZnS from single source precursor. *Solid State Sciences*, *105*, 106262. https://doi.org/10.1016/j.solidstatesciences.2020.106262

Lashgari, H., Boochani, A., Shekaari, A., Solaymani, S., Sartipi, E., & Mendi, R. T. (2016). Electronic and optical properties of 2D graphene-like ZnS: DFT calculations. *Applied Surface Science*, *369*, pp. 76–81. https://doi.org/10.1016/j.apsusc.2016.02.042

Lawal, A., Shaari, A., Ahmed, R., & Jarkoni, N. (2017a). First-principles investigations of electron-hole inclusion effects on optoelectronic properties of $Bi_2Te_3$, a topological insulator for broadband photodetector. *Physica B: Condensed Matter*, *520*, pp. 69–75. https://doi.org/10.1016/j.physb.2017.05.048

Lawal, A., Shaari, A., Ahmed, R., & Jarkoni, N. (2017b). $Sb_2Te_3$ crystal a potential absorber material for broadband photodetector: A first-principles study. *Results in Physics*, *7*, pp. 2302–2310. https://doi.org/10.1016/j.rinp.2017.06.040

Lawal, A., Shaari, A., Taura, L., Radzwan, A., Idris, M., & Madugu, M. (2021). $G_0W_0$ plus BSE calculations of quasiparticle band structure and optical properties of nitrogen-doped antimony trisulfide for near infrared optoelectronic and solar cells application. *Materials Science in Semiconductor Processing*, *124*, 105592. https://doi.org/10.1016/j.mssp.2021.105592

Li, Y., Yan, Z., & Wang, S. (2024). Spin character of interlayer excitons in tungsten dichalcogenide heterostructures: GW-BSE calculations. *Physical Review B*, *109*, *4*, 045422. https://doi.org/10.1103/PhysRevB.109.045422.

Lucarini, V., Saarinen, J. J., Peiponen, K., & Vartiainen, E. (2005). *Kramers-Kronig relations in optical materials research.* Springer. https://doi.org/10.1007/b138913

Majidiyan Sarmazdeh, M., Mendi, R. T., Mirzaei, M., & Motie, I. (2017). Investigation of the electronic and optical properties of ZnS monolayer nanosheet: First principles calculations. *Journal of Materials Science*, *52*, *6*, pp. 3003–3015. https://doi.org/10.1007/s10853-016-0555-7

Marini, A., Hogan, C., Grüning, M., & Varsano, D. (2009). yambo: An ab initio tool for excited state calculations. *Computer Physics Communications, 180,*

*8*, pp. 1392–1403. https://doi.org/10.1016/j.cpc.2009.02.003

Shahrokhi, M. (2016). Quasi-particle energies and optical excitations of ZnS monolayer honeycomb structure. *Applied Surface Science, 390*, pp. 377–384. https://doi.org/10.1016/j.apsusc.2016.08.055

Sharma, M., Mishra, D., & Kumar, J. (2019). First-principles study of the structural and electronic properties of bulk ZnS and small $Zn_nS_n$ nanoclusters in the framework of the DFT+U method. *Physical Review B, 100, 4*, 045151. https://doi.org/10.1103/PhysRevB.100.045151

Ves, S., Schwarz, U., Christensen, N. E., Syassen, K., & Cardona, M. (1990). Cubic ZnS under pressure: Optical-absorption edge, phase transition, and calculated equation of state. *Physical Review B, 42, 14*, pp. 9113–9118. https://doi.org/10.1103/PhysRevB.42.9113

Voigt, D., Sarpong, L., & Bredol, M. (2020). Tuning the optical band gap of semiconductor nanocomposites: A case study with ZnS/carbon. *Materials, 13, 18*, 4162. https://doi.org/10.3390/ma13184162

Wu, A., Qiao, Y., & Lv, F. (2016). Study on the electronic structures of ZnS and Ag-doped ZnS from density functional theory. In *ICSMIM 2015* (pp. 920–924). Atlantis Press. https://doi.org/10.2991/icsmim-15.2016.169

Yusuf, I. D., Suleiman, A. B., Lawal, A., Ndikilar, C. E., Taura, L., Gidado, A., & Chiromawa, I. M. (2024). Significant improvement in structural, electronic, optical and thermoelectric properties of $PdTe_2$ in bulk and monolayer phase: A $G_0W_0$+ BSE approach. *Physica B: Condensed Matter, 685*, 416015. https://doi.org/10.1016/j.physb.2024.416015.

**Declaration**

**Consent for publication**

Not applicable.

**Availability of data and materials**

The publisher has the right to make the data publicly available.

**Ethical Statement**

This research was conducted entirely through computational simulations using first-principles and many-body perturbation theory methods. No human participants or animals were involved. All authors contributed voluntarily, maintained scientific integrity, and have been appropriately acknowledged.

**Competing interests**

The authors declare no conflicts of interest. This work was a collaborative effort among all authors.

**Funding**

This research did not receive any external funding.

**Authors' Contributions**

I.B.U. conceptualized the study, carried out the DFT and MBPT calculations, and prepared the initial manuscript draft. A.M. contributed to data analysis, interpretation of electronic and optical properties, and manuscript revision. A.L. assisted in theoretical validation, literature review, and proofreading. All authors discussed the results and approved the final manuscript.